THE IMPACT OF PRE-ANNEALING TEMPERATURE ON THE PERFORMANCE OF Sb2S3 FILM IN PLANAR SOLAR CELL STRUCTURE

M.A. Farhana[1,2] and J. Bandara[1]

[1] National Institute of Fundamental Studies, Hantana Road, Kandy, Sri Lanka
[2] Department of Physical Sciences, South Eastern University of Sri Lanka, Sri Lanka

jayasundera.ba@nifs.ac.lk

ABSTRACT: *Sb_2S_3 has recently been widely used as a light-harvesting material in thin-film solar cells due to its exciting optical and electrical properties. Various strategies such as different precursor solutions and vacuum and non-vacuum deposition have been used to enhance the photovoltaic properties. Since the temperature impacts the optical absorption and crystallization of Sb_2S_3 films, the performance of the devices could be improved by the annealing temperature. This work aims to investigate the solar cell's performance based on pre-annealing temperature. In this work, the Sb_2S_3 precursor was prepared by dissolving thiourea and $SbCl_3$ in 2-methoxyethanol and spin-coated on a dense compact TiO_2 (c-TiO_2) layer at 4000 rpm for 30 s. Coated Sb_2S_3 films were pre-annealed at 155, 170, 185, and 200°C for 1 minute. After getting cool down, these thin films were annealed at 280°C for 10 mins in the tube furnace under the N_2 stream. This system used compact TiO_2 and P3HT as electron and hole transport materials, respectively. By increasing the annealing temperature, the devices were analyzed using UV-Vis absorption spectroscopy, Current Density-Voltage (J-V) measurement, Incident Photon to current conversion efficiency (IPCE), X-ray diffraction (XRD), and Impedance (EIS). The well-defined crystallization structure (Stibnite) of Sb_2S_3 was obtained in our study. The photovoltaic parameters were enhanced by increasing the pre-annealing temperature up to 185°C as 10.6-14.2 mA/cm^2 of Jsc, 433-526.1 mV of Voc, and 31-41% of FF. The IPCE spectra were in very good agreement with the short circuit current of the devices, showing the highest EQE of 55%, and the series and charge transfer resistances data supported the performance changes with pre-annealing temperature. The performance of the Sb_2S_3 solar cell can preciously be controlled by pre-annealing temperature, due to changes in optical and electrical properties and the device fabricated at 185°C harvested the sunlight effectively with 3.04% of efficiency.*

Keywords: absorbance, crystallization, pre-annealing, Sb_2S_3

1. INTRODUCTION

Inorganic semiconductor materials are widely used as an efficient light-harvester due to their merit properties such as having high extinction coefficient and charge carrier mobility, large intrinsic dipole moments, a wide range of optical absorption, and desirable bandgap. By changing the particle size the bandgap can be adjusted [1-3]. Sb_2S_3 is one of the chalcogenide binary compounds with a single stable phase. It is effectively used as a light-harvesting (absorbing) layer in solid-state solar cells. As the carrier diffusion length of Sb_2S_3 is in hundreds of nanometer scales, therefore, it's used in both planar and sensitized mesoporous structure device configurations [4-5]. In Sb_2S_3, the conduction bandwidth is broader than the valance band, therefore, hole mobility is less than electron mobility due to the self-trapped holes [6]. Both extrinsic surface trapping and intrinsic self-trapping can affect the device's performance due to the large area in the sensitized solar cell [7]. Since the Sb_2S_3 solar cells reached less than 8% efficiency, there are many possibilities to improve the efficiency.

The Sb_2S_3 cells are fabricated by various techniques such as chemical bath deposition (CBD), spin coating, atomic layer deposition (ALD), electrochemical deposition, vertical vapor transport (VTD), etc. Every method has its advantages and disadvantages [8-10]. Depending on the deposition techniques and conditions, the films are produced with different qualities. The controlled morphology and crystallinity of the films could lead to better performance of the solar cells.

Since the Sb_2S_3 has a low melting point (~550^{o}C), the high crystalline Sb_2S_3 films can be synthesized in low-temperature conditions. Since the crystallized Sb_2S_3 exhibits higher carrier mobility and density compared to amorphous, as-prepared Sb_2S_3 films required an additional annealing process for crystallization in many works. In a study, using the XRD pattern of Sb_2S_3 films in various temperatures it was found that the crystallization process of Sb_2S_3 occurs from 250 to 300 ^{o}C [11]. While in other studies, the optimal crystallization was reported to be at 260 and 270 ^{o}C and above 300 ^{o}C, the formation of the Sb_2O_3 layer has been reported [12-13]. The changes in annealing temperature and the time play an important role in the crystallinity changes and surface morphology as well. Nevertheless, the active layer quality and the interface energy band alignment are important factors for planar Sb_2S_3 solar cells.

In this work, solar cells of FTO/TiO_2/Sb_2S_3/P3HT/Ag configuration were prepared by a spin coating method and annealed at various pre-annealing temperatures under the N_2 stream. By controlling the important properties of Sb_2S_3 films, solar cells were developed.

2. METHODOLOGY

Electron Transport Layer (ETL) preparation: A 50 μl of di-ethanolamine aliquot was added to 910 μl of butan-1-ol and stirred for 10 minutes followed by adding 75 μl of Titanium (IV) isopropoxide (TTIP) to form 0.25 mM TiO_2 precursor solution, which can be used for a few days by proper sealing. A 30 □l of TiO2 precursor solution was spin-coated on cleaned FTO glasses at 3000 rpm for 30 s to prepare 1 cycle of the film and the thickness of the compact layer was varied by multiple TiO2 coating cycles. After every spinning cycle, the TiO2 films were heated on the hot plate at 180oC for 5 minutes and finally followed by sintering inside the box furnace at 500oC for 1 hour with 1 hour of ramping and followed the natural cooling.

Sb2S3 layer preparation: 114 mg of thiourea (TU) was dissolved in 1 ml of 2-methoxyethanol by magnetic stirring to which 228 mg of SbCl3 was added to the prepared TU solution to form a clear yellow colour solution. A 25 □l of Sb2S3 solution was spin-coated on the TiO2 ETL layer at 4000 rpm for 30 s. The spin-coated cells were heated in the tube furnace with N2 gas at 155, 170, 185, and 200oC for 1 minute with a ramping of 30 minutes and allowed to cool under natural conditions. After getting cool down, again they were annealed in the tube furnace at 280oC for 10 minutes under the N2 stream.

Hole Transport Layer (HTL) Preparation: A 2 mg of P3HT was dissolved in 100 □l of chlorobenzene and the prepared P3HT solution was used to spin coat on the Sb2S3 layers at 3000 rpm for 30 s. The coated cells were heated on the hotplate at 100oC for 20 minutes under air.

Finally, by depositing 70 nm of silver (Ag) film on the HTL by thermal evaporation method to complete the solar cells' fabrication.

The X-ray diffraction (Rigaku Ultima IV X-ray diffractometer) was used to characterize the crystal structure. The sweep range was 10-80^o and the scanning speed was 5^o/min. The optical absorption was obtained using a UV-Vis spectrophotometer (Shimadzu 2450) at 400-800 nm wavelength. The current density-voltage (J-V) measurement was done under one sunlight illumination 100 mW cm^{-2} with AM 1.5 spectral filter using a computer-controlled multi-meter

(Keithley 2000) coupled with a potentiostat unit (HA-301). The EIS measurements were obtained by using Autolab potentiostat/galvanostat PGSTAT128N with FRA 32M frequency response analyzer (Metrohms) under the illumination of 100 mW cm^{-2} with AM 1.5 spectral filter in the frequency range from 0.01 Hz to 1 MHz. The obtained data were fitted with an equivalent circuit and analyzed with the help of the software NOVA1.11.

3. RESULTS AND DISCUSSION

Figure 1 shows the X-ray diffraction patterns of Sb_2S_3 films on the FTO glass. Since the FTO has a strong crystal structure, it dominates the XRD pattern of Sb_2S_3. The crystal structure of Sb_2S_3 was confirmed by the XRD, and diffraction peaks at 15.65°, 17.54°, 25.04°, 29.26°, 32.37°, 33.42°, 46.84°, 54.45°, 64.71°, and 71.24° could be indexed to orthorhombic stibnite structure crystal planes of (200), (201), (103), (211), (212), (013), (015), (603), (712), and (803) respectively. These peaks well matched with the standard diffraction peaks (Entry #01-073-0393). However, the peak intensity is different for Sb_2S_3 film for different temperatures. Since the increasing intensity of the peaks implies an improvement in crystalline quality, the crystallinity of Sb_2S_3 films was enhanced by the increasing pre-annealing temperature. The diffraction peaks (103), (211), and (212) are stronger at 185/280°C compared to others. Therefore, the Sb_2S_3 film exhibits a strong stibnite Sb_2S_3 phase at 185/280°C, however, the plane (103) is the most preferred orientation in all samples. And also, some Sb_2O_3 peaks appeared in our samples but, most of them overlap the FTO and Sb_2S_3 peaks, which could not significantly affect the samples.

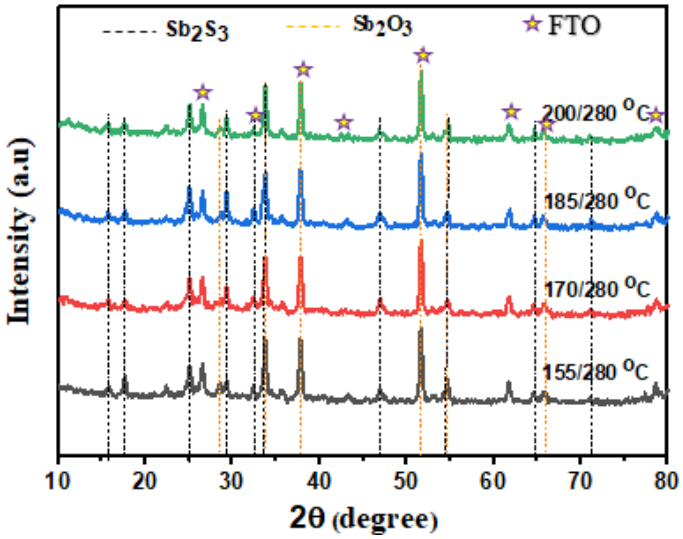

Figure 1. XRD pattern of Sb_2S_3 films in various pre-annealing temperature conditions.

The UV-Vis absorption spectra for the Sb_2S_3 films are shown in figure 2(a) and the corresponding Tauc plots are shown in figure 2(b). The Sb_2S_3 films with only the pre-annealing temperatures exhibited an amorphous nature. By heating at 280°C after pre-annealing, the films exhibited a wide range of absorbance in the visible region (400-800 nm). The energy bandgaps (Eg) of Sb_2S_3 films were obtained from the Tauc plot and the values are summarized in table 1. Increasing the temperature reduces Eg due to the increasing crystallinity. In our samples, the Eg of Sb_2S_3 films is varying from 1.65 to 1.74 eV, which is very close to the literature value (~1.7 eV).

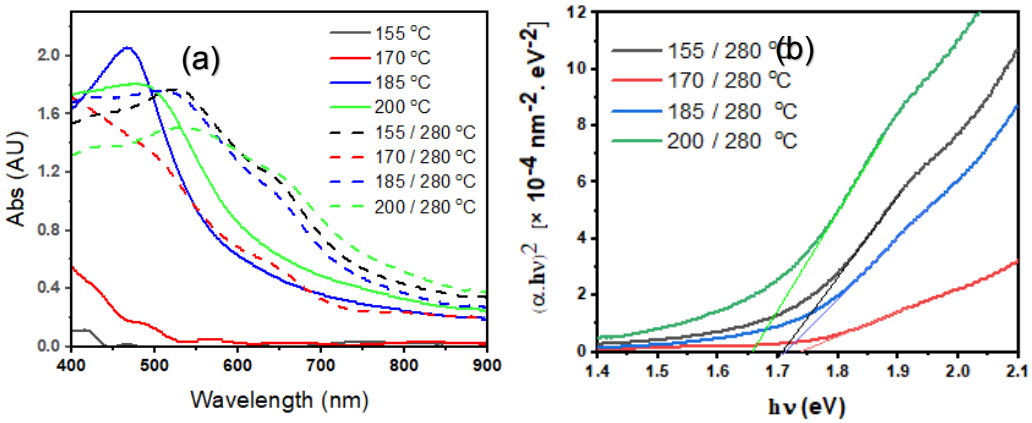

Figure 2. Optical absorption spectra for Sb_2S_3 films (a) and $(\alpha h\nu)^2$ versus $(h\nu)$ graph for Sb_2S_3 films (b) in different pre-annealing temperature treatments.

At low annealing temperatures, Sb_2S_3 films are in the poor crystalline form of the films. In this study, the films were heated in two steps as described in the methodology section. At 155°C of pre-annealing, the coated Sb_2S_3 film was not completely converted into a crystalline Sb_2S_3 film. Therefore, by the post-annealing at 280°C, the Sb_2S_3 film could produce an impurity other than Sb_2S_3. The impurities could provide a considerably higher absorbance in the visible region. The spectra show two absorbance peaks at 550 and 650 nm with the post-annealing, which are attributed crystalline and polycrystalline nature of Sb_2S_3 films, respectively [6, 14]. By increasing the pre-annealing temperature from 170 to 185°C, the absorptions were increased while decreasing at 200°C. From the absorption peaks, it was noted that at 200°C, the absorption was less in the range of 400-600 nm and higher above 600 nm compared to 185°C. It implies the polycrystalline nature was enhanced and crystalline was reduced at 200°C.

Table 1. The obtained bandgap (Eg) and thickness of the Sb_2S_3 layer with different pre-annealing temperatures.

Annealing temperature (°C)	Bandgap (eV)
155/280	1.70
170/280	1.74
185/280	1.71
200/280	1.65

Figure 3 (a) shows the J-V characteristics curves of the devices with different pre-annealing temperatures and the photovoltaic parameters are summarized in Table 2. The increasing pre-annealing temperature could make a variation in the specific electronic structure of the system. Therefore, the photovoltaic parameters are improved. In poor crystalline temperatures, the films produce in-homogeneity with small grain sizes. But, in recrystallization, even though the crystallites are enlarged by increasing annealing temperature, above an annealing temperature, the crystal islands are produced, which can be associated with decreasing device performance by reducing Voc and FF. A large number of grain boundaries could enhance the recombination [15-16].

ISBN: 978-955-627-013-6

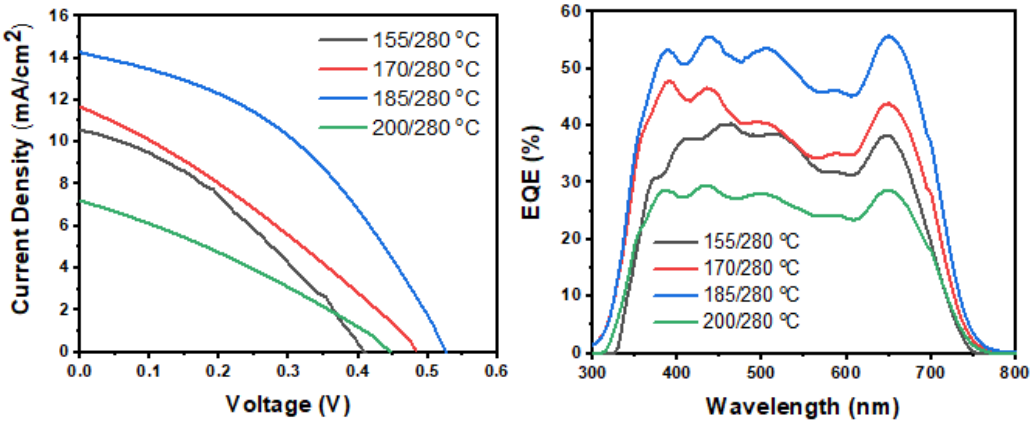

Figure 3. The Sb_2S_3 films were fabricated at different pre-annealing temperatures; J-V (a) and EQE (b) curves of the devices.

Table 2. The photovoltaic parameters of the devices at various pre-annealing temperatures under an N_2 environment.

Annealing temperature (°C)	Voc (mV)	Jsc (mA/cm^2)	FF (%)	PCE (%)
155/280	433.5	10.6	32.5	1.49
170/280	493.0	11.6	31.0	1.77
185/280	526.1	14.2	41.0	3.04
200/280	456.0	7.2	30.0	0.98

The device with Sb_2S_3 at 185/280°C exhibited higher efficiency to be 3.04% including 14.2 mA/cm^2 of Jsc, 526.1 mV of Voc, and 41% of FF. The efficiency of 0.98% was obtained at 200/280oC, it showed a rapid drop by fewer values of 7.2 mA/cm2 and 30% of Jsc and FF, respectively. The device performance at 185oC is 2 and 3 times greater than the devices at 155 and 200oC, respectively. The EQE responses of the devices are shown in figure 3 (b). The light response is considerably greater in the device fabricated at 185oC compared to others. It was nearly 55% of EQE. The UV-Vis absorption spectra are well correlated with EQE spectra from 170 to 185oC. Even though the device fabricated at 200/280oC showed a considerable absorbance, the EQE is very less. It implies that all the carriers are not effectively converted into the current at 200/280oC.

The Nyquist plots of the devices with various annealing temperatures are shown in figure 4 and the equivalent circuit used to fit the data is shown in the inset in figure 4. All the devices showed the typical semi-circle pattern. There, Rs represents ohmic series resistance associated with the resistance on FTO and external circuits while R_1 and R_2 are charge transfer resistances at the interfaces of Sb_2S_3/P3HT and Sb_2S_3/TiO_2.

ISBN: 978-955-627-013-6

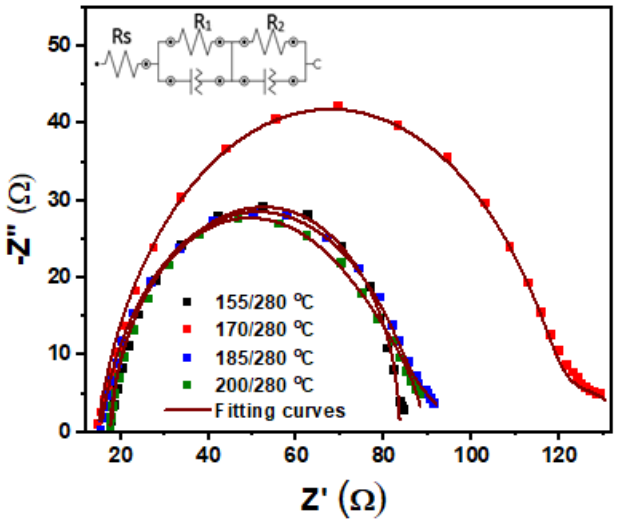

Figure 4. The impedance curves of the devices at various pre-annealing temperatures.

The impedance parameters were obtained from the fitted equivalent circuits and summarized in table 3. The reducing Rs values showed excellent ohmic contact with the FTO substrate while charge transfer resistance enhances the charge extraction between the phases. Reducing R_1 and R2 could reduce the recombination.

When increasing the annealing temperature from 170 to 200°C, the Rs values were increased and R_2 values were decreased while R_1 values fluctuated. Nevertheless, the contribution of all Rs, R_1, and R_2 influence the device performance. The device at 185°C exhibited better performance with significant contributions of Rs, R_1, and R_2.

Table 3. EIS parameters of the devices with various pre-annealing temperatures of Sb_2S_3 films in N_2.

Annealing temperature (°C)	Rs (Ω)	R_1 (Ω)	R_2 (Ω)
155/280	17.8	15.4	49.5
170/280	14.6	16.8	104
185/280	15.4	9.11	70.4
200/280	17.5	14.9	57.0

4. CONCLUSION

The annealing temperature of Sb_2S_3 film highly influences solar cell performance. By applying a proper annealing condition, the optical and electrical properties of the films could be controlled. Our investigation exhibited that the pre-annealing temperature has a significant effect on both the optical absorption and crystallinity of Sb_2S_3 films. By optimizing the pre-annealing temperature, the highest photovoltaic performance of 3.04% was at 185°C under N_2 gas. Since the pre-annealing temperature affects the performance, future work can be done based on annealing time, environment, etc.

REFERENCES

[1] Bansal, N., O'Mahony, F. T. F., Lutz, T., & Haque, S. A. (2013). Solution Processed Polymer-Inorganic Semiconductor Solar Cells Employing Sb2S3 as a Light Harvesting and Electron Transporting Material. *Advanced Energy Materials,* 3(8), 986–990.

[2] Dong, C. R., Wang, Y., Zhang, K., & Zeng, H. (2020). Halide perovskite materials as light harvesters for solar energy conversion. *EnergyChem,* 100026.
[3] Boix, P. P., Nonomura, K., Mathews, N., & Mhaisalkar, S. G. (2014). Current progress and future perspectives for organic/inorganic perovskite solar cells. *Materials Today,* 17(1), 16–23.
[4] Zhou, H., Han, J., Pu, X., & Li, X. (2021). Effective additive for enhancing the performance of Sb2S3 planar thin film solar cells. *Journal of Materiomics,* 7(5), 1074–1082.
[5] Choi, Y. C., Lee, D. U., Noh, J. H., Kim, E. K., & Seok, S. I. (2014). Highly Improved Sb2S3Sensitized-Inorganic-Organic Heterojunction Solar Cells and Quantification of Traps by Deep-Level Transient Spectroscopy. *Advanced Functional Materials,* 24(23), 3587–3592.
[6] Yang, Z., Wang, X., Chen, Y., Zheng, Z., Chen, Z., Xu, W., … Zhu, H. (2019). Ultrafast self-trapping of photoexcited carriers sets the upper limit on antimony trisulfide photovoltaic devices. *Nature Communications,* 10(1), 1-8.
[7] Christians, J. A., Leighton, D. T., & Kamat, P. V. (2014). Rate limiting interfacial hole transfer in Sb2S3 solid-state solar cells. *Energy Environ. Sci.,* 7(3), 1148–1158.
[8] Grad, L., von Rohr, F. O., Hengsberger, M., & Osterwalder, J. (2021). Charge carrier dynamics and self-trapping on Sb2S3(100). *Physical Review Materials,* 5(7).
[9] Sung, S.-J., Gil, E. K., Lee, S.-J., Choi, Y. C., Yang, K.-J., Kang, J.-K., … Kim, D.-H. (2017). Systematic control of nanostructured interfaces of planar Sb 2 S 3 solar cells by simple spin-coating process and its effect on photovoltaic properties. *Journal of Industrial and Engineering Chemistry,* 56, 196–202.
[10] Zhang, H., Yuan, S., Deng, H., Ishaq, M., Yang, X., Hou, T., … Tang, J. (2020). Controllable orientations for Sb 2 S 3 solar cells by vertical VTD method. *Progress in Photovoltaics: Research and Applications.*
[11] Wang, X., Li, J., Liu, W., Yang, S., et al. (2017). A Fast Chemical Approach towards Sb2S3 Film with Large Grain Size for High-Performance Planar Heterojunction Solar Cells. *Nanoscale,* 9(10), 3386-3390.
[12] Sun, R.-D., & Tsuji, T. (2015). Preparation of antimony sulfide semiconductor nanoparticles by pulsed laser ablation in liquid. *Applied Surface Science,* 348, 38–44.
[13] Parize, R., Cossuet, T., Chaix-Pluchery, O., Roussel, H., Appert, E., & Consonni, V. (2017). In situ analysis of the crystallization process of Sb 2 S 3 thin films by Raman scattering and X-ray diffraction. *Materials & Design,* 121, 1–10.
[14] Dong, W., et al. (2019). Wide bandgap phase change material tuned visible photonics. *Advanced Functional Materials*, 29(6), 1806181.
[15] Pan, G., Wang, D., Gao, S., Gao, P., Sun, Q., Liu, X., … Zhang, Y. (2019). Substrate structured Sb2S3 thin film solar cells fabricated by rapid thermal evaporation method. *Solar Energy,* 182, 64–71.
[16] Liu, C. P., Wang, H. E., Ng, T. W., Chen, Z. H., Zhang, W. F., Yan, C., … Jha, S. K. (2011). Hybrid photovoltaic cells based on ZnO/Sb2S3/P3HT heterojunctions. *Physica Status Solidi (b),* 249(3), 627–633.